1995ApJ...454..447Z

THE ASTROPHYSICAL JOURNAL, 454:447–462, 1995 November 20
© 1995. The American Astronomical Society. All rights reserved. Printed in U.S.A.

THE 71 SECOND OSCILLATION IN THE LIGHT CURVE OF THE OLD NOVA DQ HERCULIS

E. ZHANG AND E. L. ROBINSON
Department of Astronomy, University of Texas, Austin, TX 78712; erho,elr@astro.as.utexas.edu
R. F. STIENING
Department of Physics and Astronomy, University of Massachusetts, Amherst, MA 01002; stiening@cannon.phast.umass.edu
AND
KEITH HORNE
School of Physics and Astronomy, University of St. Andrews, North Haugh, St. Andrews, Fife KY16 9SS, Scotland, UK; kdh1@st-andrews.ac.uk
Received 1995 March 9; accepted 1995 May 31

ABSTRACT

DQ Her is an old nova (N1934), an eclipsing binary with an orbital period of 0.1936 days, and a prototype for cataclysmic variables containing rapidly rotating, accreting, magnetic white dwarfs. We have obtained high-speed, simultaneous U, B, V, and R photometry of DQ Her and have used the photometry to update and improve the ephemerides for the eclipse and for the 71 s periodicity induced by the rotation of the white dwarf. We use the ephemerides to show that the present rate of mass transfer in DQ Her must be less than, but not much less than $3.4 \times 10^{-9}\ M_\odot\ \mathrm{yr}^{-1}$ and that the magnetic moment of the white dwarf is near $2.7 \times 10^{32}\ \mathrm{G\ cm}^3$.

The mean fractional semiamplitudes of the 71 s oscillation just before eclipse are $\Delta U/U = 0.010 \pm 0.001$, $\Delta B/B = 0.012 \pm 0.001$, $\Delta V/V = 0.011 \pm 0.001$, and $\Delta R/R = 0.009 \pm 0.001$. The large change in oscillation amplitude with orbital phase seen in earlier data is no longer present. The 71 s oscillation undergoes a phase shift during eclipse, and we give a much improved measurement of the shift. The phase increases smoothly by at least 100° during eclipse ingress, then jumps by 120° at mid-eclipse, and finally climbs smoothly by another 140° during eclipse egress to end at +360°. The morphology of the phase shift is not measurably different in the four passbands. The beamed radiation from the white dwarf in DQ Her irradiates its accretion disk, setting up a pattern of bright and dark regions that rotates with the white dwarf. We show that the pattern has two nearly equal bright regions in opposite directions on the disk and that the pattern rotates with a period of 142 s. The rotation period of the white dwarf is, thus, 142 s.

Subject headings: binaries: eclipsing — novae, cataclysmic variables — stars: individual (DQ Herculis) — stars: oscillations — stars: rotation — white dwarfs

1. INTRODUCTION

The old nova DQ Herculis (N1934) is an eclipsing binary star with an orbital period of 4^h39^m consisting of a cool star with a mass near 0.4 $M_\odot$, presumed to be on the main sequence, and a white dwarf with a mass near 0.6 $M_\odot$ (Horne, Welsh, & Wade 1993). The cool star is transferring mass through the inner Lagrangian point to the white dwarf. Kraft (1959) discovered that the He II emission line at 4686 Å displays a classical rotational disturbance during eclipse, thus demonstrating that the transferred gas forms a rotating disk around the white dwarf, the first direct evidence for an accretion disk in a cataclysmic variable. The flux from DQ Her at visible wavelengths is dominated by the accretion disk; the white dwarf is never visible, and the cool star is visible only when it eclipses the disk.

DQ Her is a prototype for cataclysmic variables in which the white dwarf is rapidly rotating and has a strong magnetic field (see Patterson 1994). Gas accreting onto the white dwarf in these systems threads onto the magnetic field lines and falls onto the white dwarf at one or both magnetic poles, where the sudden release of kinetic energy forms highly luminous spots. The rotation of the white dwarf produces a modulation of the light curve, which in DQ Her is at a period of 71.06 s. This 71 s modulation was first found by Walker on 1954 July 9 (Walker 1956) and has been studied extensively ever since, but many of its basic properties are not yet well established. Its ephemeris has been plagued by an uncertain cycle count during the interval from 1959 to 1967, when DQ Her was not observed (Patterson, Robinson, & Nather 1978 [hereafter PRN]; Balachandran, Robinson, & Kepler 1983). Furthermore, although there is no compelling evidence that any observable property of DQ Her is modulated at 142 s (e.g., Kiplinger & Nather 1975), there has been a persistent suspicion that the true period of DQ Her could be 142 s, not 71 s.

Warner et al. (1972) found that the times of maxima of the 71 s oscillation occur progressively earlier during the eclipse until mid-eclipse and then return to their normal phase as eclipse ends. Although the 71 s oscillation must originate in the white dwarf, the long duration of this eclipse phase shift demonstrates that the observed oscillation comes from the accretion disk, not the white dwarf. The similarity of the oscillation color to the mean color of DQ Her supports this conclusion (PRN). Flux from the spotted white dwarf, which is rotating in the prograde direction, irradiates the accretion disk, forming a pattern of bright and dark spokes that sweep azimuthally around the disk (PRN; Chester 1979; Petterson 1980). The positive sign of the phase shift shows that the pattern is visible only from the back of the disk, so that progressive occultation of the disk during eclipse ingress causes the maximum visibility of the pattern to occur earlier in its sweep across the disk. The

© American Astronomical Society • Provided by the NASA Astrophysics Data System

1995ApJ...454..447Z

existing data suggest that the pattern has one spoke and a rotation period of 71 s, but a two-spoked pattern with a rotation period of 142 s has not been ruled out. The ambiguity arises because interpretation of the phase shift depends strongly on the morphology of the phase shift near mid-eclipse, precisely when the amplitude of the oscillation is small and the phase is poorly determined.

In this paper we present new, multicolor, high-speed photometry of the light curve of DQ Her. We use the photometry to improve the ephemerides for the time of eclipse and the 71 s oscillation. We also give an improved measurement of the eclipse phase shift and show that a two-spoked pattern fits the data better than a one-spoked pattern. The two-spoked pattern implies that the true rotation period of the white dwarf is 142 s.

2. OBSERVATIONS

The new observations of DQ Her were obtained with the Stiening high-speed photometer. This photometer uses dichroic beam splitters to obtain simultaneous measurements of the stellar flux in four passbands roughly similar to the passbands of the Johnson *UBVR* system. Plots of the four response functions and a table with their effective wavelengths and FWHMs can be found in Robinson et al. (1995). We observed DQ Her in 1982 with the 1.5 m telescope at Mount Palomar, in 1983 with the 1.5 m telescope at Mount Lemmon, and in 1991, 1992, and 1994 with the 2.1 m telescope at McDonald Observatory, typically with a 1 s time resolution (see Table 1). Corrections for sky background and extinction were made in the usual ways. The reduced light curves from run 302 (1991 May 9) are shown in Figure 1.

The Johnson magnitudes and colors of DQ Her out of eclipse and at eclipse minimum are given in Table 2, where we have used Walker's (1956) comparison stars B and C to derive an approximate transformation from Stiening magnitudes to Johnson magnitudes. The magnitudes in 1983 are the means from runs 419 to 436; and the magnitudes in 1991 to 1994 are the means from runs 300, 302, 398, and 525 for the magnitudes out of eclipse and from run 398 for the magnitudes at eclipse minimum. Because of the conversion between magnitude systems and because of the intrinsic variability of DQ Her, the Johnson magnitudes are not more accurate than ± 0.1 magnitude.

TABLE 1

PHOTOMETRIC OBSERVATIONS OF DQ HERCULIS

Run	Start Time (UTC)	Integration Time (s)	Length (s)	Filters	Telescope
345.....	1982 Sep 21 3:31:31	1.0	8192	*UBR*	1.5 m
349.....	1982 Sep 22 2:40:51	1.0	8192	*UBR*	1.5 m
416.....	1983 Sep 14 4:56:54	1.0	4757	*UBVR*	1.5 m
418.....	1983 Jun 14 9:23:31	1.0	4784	*UBVR*	1.5 m
419.....	1983 Jun 15 4:04:03	1.0	6660	*UBVR*	1.5 m
421.....	1983 Jun 15 8:09:57	1.0	7396	*UBVR*	1.5 m
423.....	1983 Jun 16 7:53:39	1.0	6007	*UBVR*	1.5 m
426.....	1983 Jun 17 7:02:43	1.0	7068	*UBVR*	1.5 m
429.....	1983 Jun 18 6:13:42	1.0	6719	*UBVR*	1.5 m
436.....	1983 Jun 21 8:16:38	1.0	8192	*UBVR*	1.5 m
300.....	1991 May 8 6:03:04	0.5	16000	*UBVR*	2.1 m
302.....	1991 May 9 6:10:11	0.5	16000	*UBVR*	2.1 m
398.....	1992 Jun 3 4:53:42	1.0	17144	*UBVR*	2.1 m
518.....	1994 May 4 7:44:58	1.0	10681	*UBVR*	2.1 m
525.....	1994 May 5 6:14:50	1.0	13866	*UBVR*	2.1 m

TABLE 2

MEAN JOHNSON MAGNITUDES

Year	Orbital Phase	*V*	*B*−*V*	*U*−*B*
1983	Out of Eclipse	14.37	+0.20	−0.71
	Eclipse Minimum	16.81	+0.19	−0.89
1991–1994.....	Out of Eclipse	14.56	+0.26	−0.70
	Eclipse Minimum	17.12	+0.39	−0.74

Figure 2 shows the mean *B* magnitude and the depth of the eclipse in DQ Her as a function of time. The magnitudes have been taken from our Table 2 and from Table 2 in PRN; the magnitudes from PRN are seasonal averages for those years with more than one measurement. DQ Her faded by ~ 0.6 mag in *B* between 1954 and 1975 but has remained roughly constant since then. The eclipse depth in *B* has increased by a large amount, from ~ 1.0 mag in 1954 to ~ 2.7 mag in 1992. Thus, the fraction of *B* flux from DQ Her that is uneclipsed has decreased from $\sim 40\%$ to $\sim 9\%$. The change in the *U* eclipse depth follows the change in *B* closely, but in *V* the eclipse deepened only until 1977 and has remained roughly constant since then.

Figure 3 compares the eclipse light curve measured by Walker (1958) on 1955 May 16 to the light curve we measured on 1991 May 9. The 1955 light curve has been converted to intensity units and normalized to the 1991 light curve at the orbital phases just before eclipse. The change in eclipse depth is striking. Figure 3 also shows the 1955 light curve after subtraction of a constant background flux. The subtracted 1955 light curve departs greatly from the 1991 light curve between orbital phases 0.08 and 0.16 but otherwise the two light curves are similar. The eclipse width and the slopes of the ingress and egress match each other well, demonstrating that neither the size nor the brightness distribution across the accretion disk has changed greatly. Thus, the increase in the depth of the eclipse between 1955 and 1991 is primarily the result of a decrease in the uneclipsed background flux, not a change in the properties of the disk. A plausible source of the background flux is the nebula ejected when DQ Her erupted in 1934. As the nebula has faded, those parts of the nebula included in the photometer aperture have contributed less flux to the light curve.

Although neither the brightness distribution across the disk nor its size have changed greatly, they probably have changed at least somewhat. Since the fading of the nebula accounts for only about half the decrease in the flux from DQ Her out of eclipse, the total brightness of the disk may have decreased between 1955 and 1977. The difference between the 1955 and 1991 light curves at orbital phases 0.08 to 0.16 might have been caused by a large flicker in the 1955 light curve, but a more plausible explanation is that the bright spot on the edge of the disk is more prominent in the 1991 light curve and is still partially eclipsed at those orbital phases.

3. EPHEMERIDES FOR THE ECLIPSE AND FOR THE 71 SECOND OSCILLATION

3.1. *The Eclipse Ephemeris*

Our light curves provide 15 new times of minima for the eclipses of DQ Her. The heliocentric Julian ephemeris dates (HJEDs) of the eclipse minima were determined by the method of bisecting cords and have an internal accuracy of ± 10 s. We

© American Astronomical Society • Provided by the NASA Astrophysics Data System

1995ApJ...454..447Z

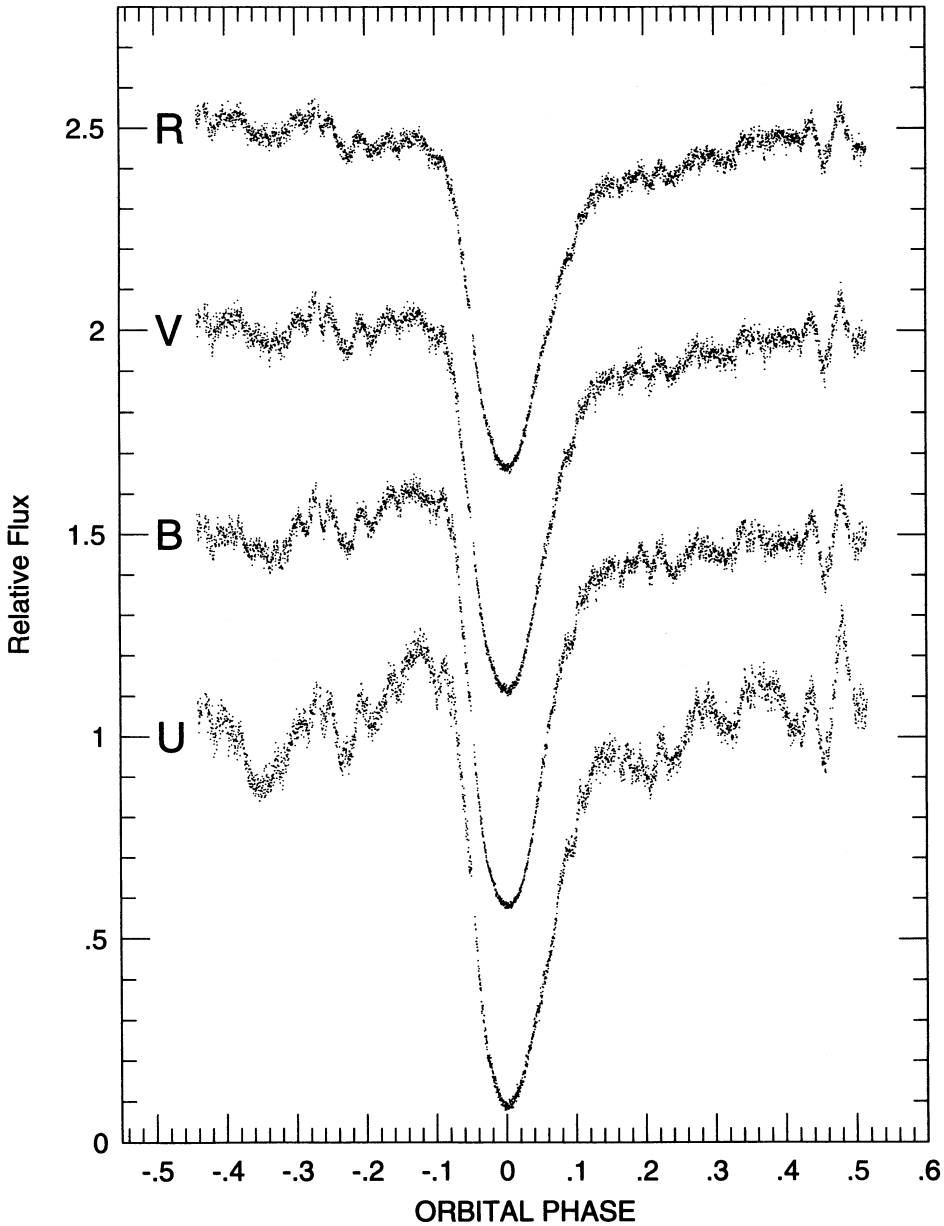

FIG. 1.—The Stiening *UBVR* light curves of DQ Her from run 302 (1991 May 9). The light curves have been normalized to 1.00 out of eclipse, and each light curve has been displaced upward to avoid overlap. The light curves have been averaged to 5 s per point.

find, in agreement with Schneider & Greenstein (1979) and Africano & Olson (1981), that the times of minimum are the same in all colors to within the accuracy of measurement and, therefore, we give eclipse times only for the *B* light curves, which have the highest signal-to-noise ratio. The new times of minima are listed in Table 3, which also includes three times from Balachandran (1983) and two from Schoembs & Rebhan (1989). After conversion to HJED, the times of minima listed by Africano & Olson (1981) yield another 88 for a total of 103 eclipse times spread over 40 years. The cycle counts for the eclipses are unambiguous. Unweighted least-squares fits to the times of minima yield the linear ephemeris

$$T_{\rm min} = \text{HJED } 2{,}434{,}954.94429(\pm 8) + 0.1936208964(\pm 12)E\ , \quad (1)$$

and the quadratic ephemeris

$$T_{\rm min} = \text{HJED } 2{,}434{,}954.94432(\pm 7) + 0.1936208935(\pm 22)E + (5 \pm 4) \times 10^{-14}E^2\ . \quad (2)$$

The $O-C$ residuals with respect to the linear ephemeris are listed in Table 3 and plotted in Figure 4.

The rms residual of the times of minima is ± 68 s, much larger than the internal accuracy of the times. Part of the scatter is caused by rapid variability in the shape of the eclipse, which introduces a scatter near ± 40 s, but the rest is caused by systematic differences between the observed and calculated times of minima. PRN and Africano & Olson (1981) found that these systematic differences are cyclic with a period near 4900 days. The cyclic variation persists in the new data. A fit of a

© American Astronomical Society • Provided by the NASA Astrophysics Data System

1995ApJ...454..447Z

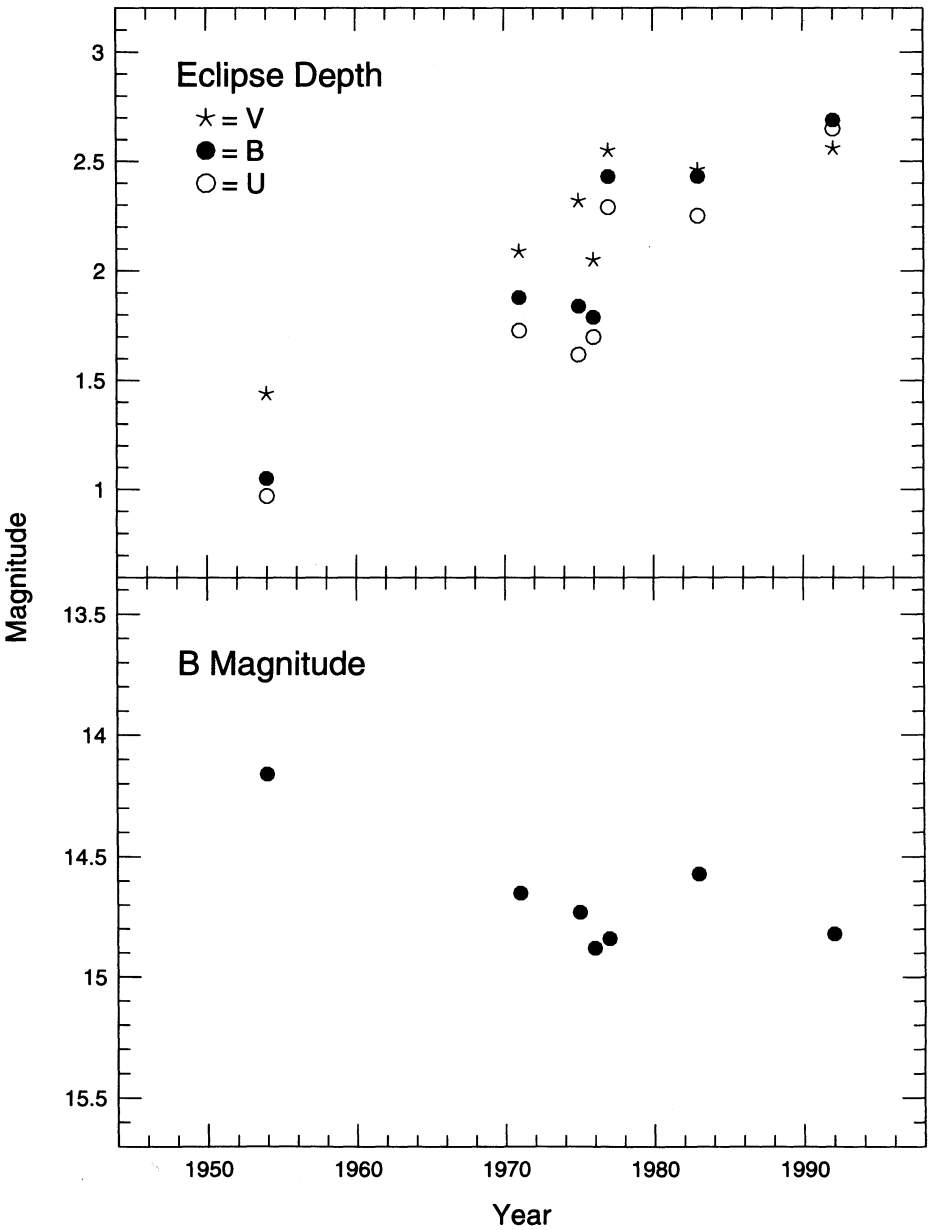

FIG. 2.—*Bottom*: mean Johnson *B* magnitude of DQ Her out of eclipse as a function of time. DQ Her faded by ~0.5 mag between 1954 and 1976 but has been nearly constant since then. *Top*: the depth of the eclipse in DQ Her in Johnson magnitudes as a function of time. In *U* and *B*, the eclipse depth increased from 1.0 mag in 1954 to 2.7 mag in 1992. In *V*, the depth increased from ~1.5 mag in 1954 to ~2.6 mag in 1977 but has not changed significantly since then.

sine curve to the residuals in the $O-C$ diagram now gives $0^d.008 \sin 2\pi\psi$, where $\psi = (T - 2{,}437{,}900)/5000$ and T is the Julian Date, in basic agreement with PRN. Applegate & Patterson (1987), Warner (1988), and Bianchini (1990) have ascribed these cyclic variations and similar variations in the orbital periods of other cataclysmic variables to solar-type magnetic cycles in the secondary stars. This mechanism would suggest that the variations in the $O-C$ diagram should be quasi-periodic, not strictly periodic, and indeed the variations in the $O-C$ diagram of UX UMa, one of the best-observed cataclysmic variables, are definitely not periodic (Rubenstein, Patterson, & Africano 1991), nor most probably are the variations in the $O-C$ diagrams of other cataclysmic variables (Richman, Applegate, & Patterson 1994). Although the variations in the $O-C$ diagram of DQ Her do appear to be more regular than those of UX UMa, it is best to consider 5000 days to be a timescale for the variations rather than a period or even a quasi-period until the observations cover more than three cycles of the variation.

The quadratic term in equation (2) is 40 times smaller than the quadratic term in the ephemeris of Africano & Olson (1981). It is now clear that the large quadratic term they found was an artifact of overfitting the systematic departures and that the skepticism they expressed about its significance was justified. Since the quadratic term in equation (2) differs from zero by only $\sim 1.2\ \sigma$ and since the statistical test proposed by Pringle (1975) shows that it has a low significance, the linear ephemeris is strongly preferred. To find an upper limit to the

© American Astronomical Society • Provided by the NASA Astrophysics Data System

1995ApJ...454..447Z

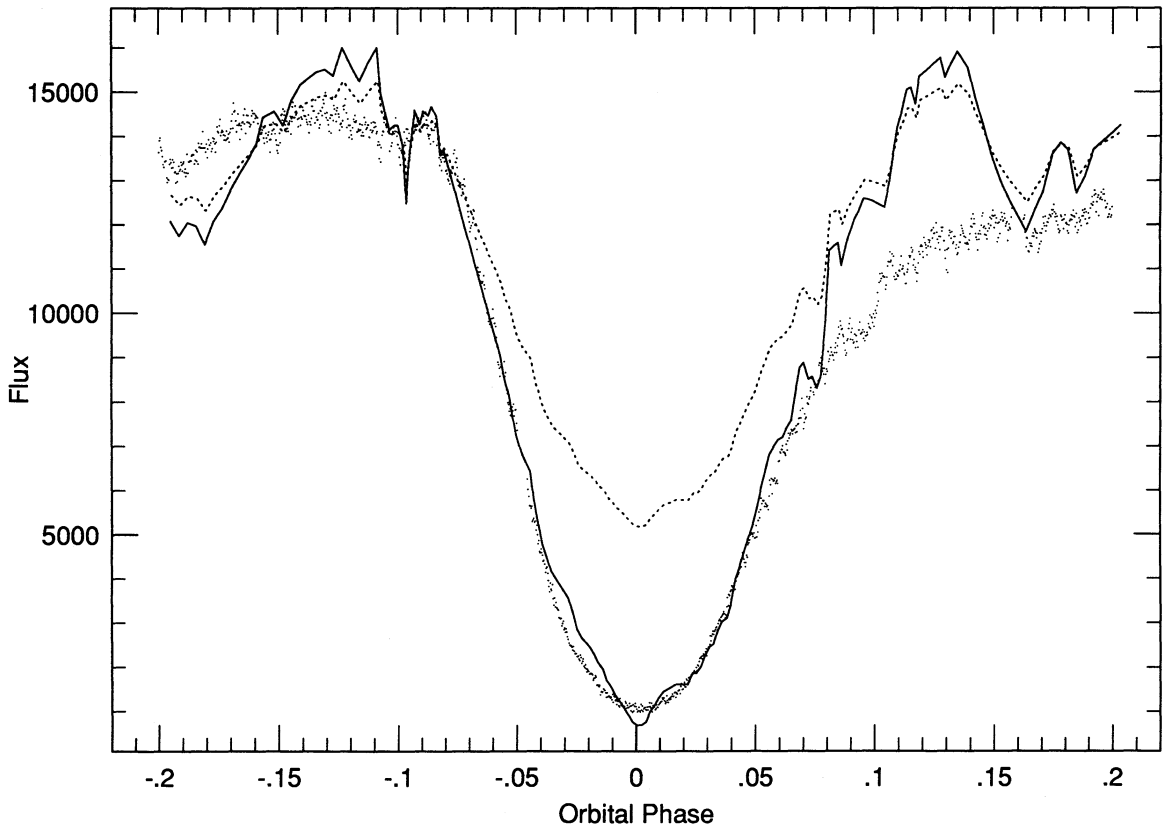

FIG. 3.—*Dots*: the blue light curve of DQ Her in 1991 (run 302). *Dashed line*: the blue light curve of DQ Her in 1955 (Walker 1958). *Solid line*: the 1955 light curve after subtraction of a constant background flux. Both the original and the subtracted 1955 light curves have been normalized to the flux in the 1991 light curve just before eclipse.

rate of change of the orbital period, we note first that the systematic departures of the timings in the $O-C$ diagram suggest that the formal standard deviation of the quadratic term seriously underestimates the true uncertainty. The error in the quadratic term was calculated assuming that the true error of an individual measurement is 10 s, but from the residuals of the fit we deduce that the true error is closer to 68 s. The standard deviation of the quadratic term scales linearly with the standard deviation of the individual measurements, and thus the true standard deviation should be 6.8 times larger than the quoted value, or 2.7×10^{-13} days. We find, then, that the upper limit to the rate of change of the orbital period is $|\dot{P}| < 4.5 \times 10^{-12}$ s s^{-1} with a 90% probability. The dashed line in Figure 4 corresponds to a quadratic ephemeris in which $|\dot{P}| = 4.5 \times 10^{-12}$ s s^{-1}. We believe this is a reliable upper limit to the rate of change of the orbital period.

TABLE 3

TIMES OF MID-ECLIPSE

HJED (2,400,000+)	Cycle Number	$O-C$ (days)
45142.8904[a]	52618	0.0018
45144.8264[a]	52628	0.0016
45203.6867[a]	52932	0.0011
45233.6976	53087	0.0008
45234.6660	53092	0.0011
45499.7322	54461	0.0003
45499.9256	54462	0.0001
45500.7004	54466	0.0004
45500.8932	54467	−0.0005
45501.8622	54472	0.0004
45502.8299	54477	0.0000
45503.7980	54482	0.0000
45506.8960	54498	0.0001
46626.6037[b]	60281	−0.0018
46627.5714[b]	60286	−0.0022
48384.8756	69362	−0.0013
48385.8440	69367	−0.0010
48776.7656	71386	0.0000
49476.8989	75002	0.0001
49477.8664	75007	−0.0005

[a] From Balachandran 1983.
[b] From Schoembs & Rebhan 1989.

As shown by Molnar (1988) and Robinson, Shetrone, & Africano (1991), if the mass-losing star in an interacting binary fills its Roche lobe and has a mass-radiation relation given by the power law $R_r \propto M_r^{\beta}$, then

$$\frac{\dot{M}_r}{M_r} = \frac{2}{3\beta - 1}\frac{\dot{P}}{P}, \tag{3}$$

where $\dot{M}_r$ is the rate of mass loss from the late-type star. Equation (3) holds even for nonconservative mass transfer. Adopting $|\dot{P}| < 4.5 \times 10^{-12}$ s s^{-1}, $\beta = 1$, and $M_r = 0.4\ M_\odot$ for DQ Her (Horne et al. 1993), we find $|\dot{M}_r| < 3.4 \times 10^{-9}\ M_\odot$ yr^{-1}. This limit is close to the rate of mass transfer derived from the strength of the Balmer emission lines (Patterson 1984). It is much less than the rate determined from the absolute magnitude of the accretion disk of DQ Her at minimum light (Warner 1987), but use of the absolute magnitude requires a large and uncertain correction for the orbital inclination of DQ Her.

© American Astronomical Society • Provided by the NASA Astrophysics Data System

1995ApJ...454..447Z

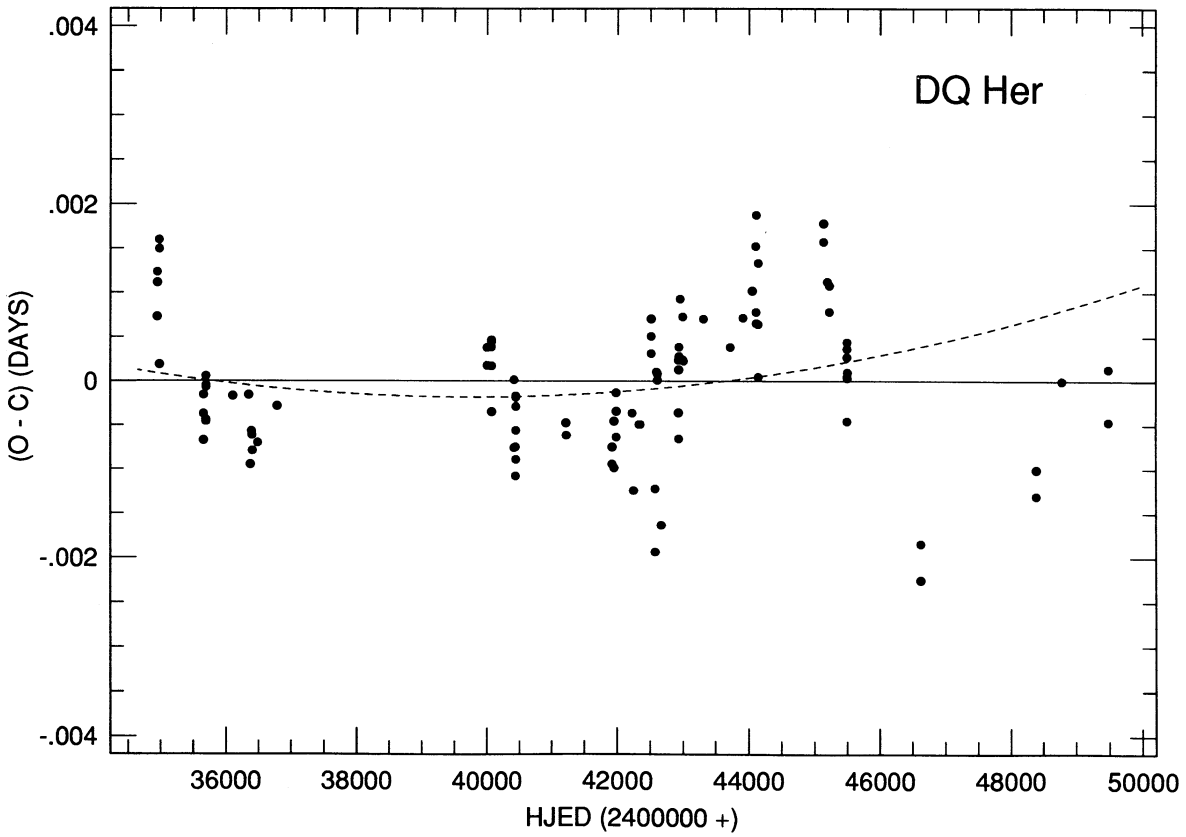

FIG. 4.—The $O-C$ diagram for the eclipses of DQ Her. The ephemeris is the linear ephemeris given in eq. (1) in the text. Dashed line shows the quadratic ephemeris in which the coefficient of the quadratic term is 4.5×10^{-13} days.

It is interesting to compare our upper limit to various theoretical estimates for the rate of mass transfer. The limit is beginning to put pressure on theoretical calculations of the evolution of cataclysmic variables. McDermott & Taam (1989), for example, summarized their calculations with the relation

$$\dot{M}_r = -1.17 \times 10^{-9}(P/3 \text{ hr})^{3.7}\, M_\odot \text{ yr}^{-1}\,, \qquad (4)$$

which for DQ Her yields $\dot{M}_r = -5.7 \times 10^{-9}\, M_\odot$ yr^{-1}. Studies of thermal instabilities in accretion disks have shown that there is a critical mass transfer rate, $\dot{M}_{\rm crit}$, below which the accretion disk becomes unstable, leading to dwarf nova eruptions. According to Shafter, Wheeler, & Cannizzo (1986), the critical accretion rate for a binary with the orbital period of DQ Her and a white dwarf mass of 0.6 $M_\odot$ is $3.5 \times 10^{-9}\, M_\odot$ yr^{-1}. Since DQ Her does not show dwarf nova eruptions, its rate of mass transfer should lie above this limit, and, thus, our upper limit to the rate of mass transfer must be close to the true rate. An observed rate of $3.4 \times 10^{-9}\, M_\odot$ yr^{-1} does not appear inconsistent with the rates required by theoretical models for the nova eruptions (Starrfield 1989). It is not clear, however, that the rate we have measured is directly comparable to the rates predicted by models for binary evolution and nova eruptions, since the present rate of mass transfer could be much larger than the mean rate (Shara 1989).

3.2. *The Ephemeris for the 71 Second Oscillation*

We have extracted a single mean time of maximum for the 71 s oscillation in each observing run by fitting sine functions to the light curve, excluding orbital phases -0.05 to $+0.05$, which are too near mid-eclipse. We could not derive a time of maximum from runs 349 and 418 because they were short and centered on the eclipse, so the 15 runs yielded 13 new times of maximum. The times have been converted to heliocentric times, not barycentric times, to maintain consistency with earlier measurements; the difference between heliocentric and barycentric times are small for DQ Her because it is only $\sim 23°$ from the north ecliptic pole.

The heliocentric Julian ephemeris dates of the times of maxima are listed in Table 4. The times of maximum are independent of color to within the measurement error and, therefore, we give the times only for the B light curves, which have the highest signal-to-noise ratio and smallest measurement error. The internal standard deviations of the times are generally less than ± 2.0 s. Table 4 also includes two unpublished times of maxima obtained with the 5 m Hale telescope by Martell et al. (1995), the 74 times published by PRN, and the 11 times published by Balachandran et al. (1983), for a total of 100 times of maxima obtained over the last 40 years. The observations cover the 40 years well except for a gap between 1959 and 1967. Since the 83 timings obtained after the gap have a unique cycle count, we have defined cycle zero to be the first cycle after the gap with a measured time of maximum.

Figure 5 shows the $O-C$ diagram for the times of maxima with respect to a linear ephemeris, and Figure 6 shows the $O-C$ diagram with respect to a quadratic ephemeris derived by fitting only the times of maxima after the gap (cycles 0 and greater). The quadratic ephemeris is clearly inadequate. The

© American Astronomical Society • Provided by the NASA Astrophysics Data System

1995ApJ...454..447Z

TABLE 4

71 SECOND OSCILLATION TIMES OF MAXIMA

Cycle Number[a]	HJED (2,400,000+)	$O-C$ (s)	Source[b]	Cycle Number[a]	HJED (2,400,000+)	$O-C$ (s)	Source[b]
−5682520.....	34954.78572	−25.6	PRN	3299489	42342.65918	1.0	PRN
−4825434.....	35659.75750	−0.4	PRN	3539413	42540.00071	5.2	PRN
−4824249.....	35660.73221	1.5	PRN	3575555	42569.72800	−3.5	PRN
−4781660.....	35695.76253	−0.9	PRN	3577866	42571.62882	−5.2	PRN
−4780483.....	35696.73058	−5.9	PRN	3578093	42571.81549	−8.6	PRN
−4779079.....	35697.88548	1.1	PRN	3578120	42571.83769	−9.8	PRN
−4285669.....	36103.72547	−1.3	PRN	3578143	42571.85660	−10.0	PRN
−4275947.....	36111.72199	−3.6	PRN	3583990	42576.66586	−9.5	PRN
−3996126.....	36341.88065	6.4	PRN	3584056	42576.72022	−3.4	PRN
−3983897.....	36351.93929	9.6	PRN	3584086	42576.74487	−5.9	PRN
−3953523.....	36376.92248	5.4	PRN	3604618	42593.63286	1.1	PRN
−3933058.....	36393.75532	1.7	PRN	3605828	42594.62809	0.0	PRN
−3925745.....	36399.77040	0.7	PRN	3648833	42630.00048	6.0	PRN
−3915865.....	36407.89693	3.0	PRN	4007220	42924.77955	−5.1	PRN
−3823738.....	36483.67330	5.4	PRN	4008458	42925.79784	−3.9	PRN
−3818876.....	36487.67243	8.4	PRN	4009704	42926.82271	−2.6	PRN
−3456370.....	36785.84102	11.4	PRN	4010930	42927.83109	−4.4	PRN
0	39628.77181	3.3	PRN	4012081	42928.77780	−5.0	PRN
157824.....	39758.58487	−2.2	PRN	4013282	42929.76566	−3.9	PRN
165053.....	39764.53080	−6.9	PRN	4281039	43150.00029	7.9	PRN
166353.....	39765.60016	0.5	PRN	4438824	43279.78086	−4.6	PRN
167452.....	39766.50416	5.0	PRN	4442489	43282.79538	−4.8	PRN
537487.....	40070.86461	0.8	PRN	4442566	43282.85871	−5.1	PRN
843870.....	40322.87019	6.0	PRN	4476472	43310.74701	0.1	PRN
959341.....	40417.84702	−5.4	PRN	5372573	44047.80430	−5.4	BRK
960490.....	40418.79215	−0.4	PRN	5372596	44047.82322	−5.6	BRK
988488.....	40441.82099	−1.6	PRN	5381028	44054.75868	−5.0	BRK
989685.....	40442.80553	−2.7	PRN	5381043	44054.77094	−11.9	BRK
990853.....	40443.76622	−3.6	PRN	6702681	45141.83883	5.3	BRK
992000.....	40444.70968	−1.2	PRN	6702711	45141.86354	8.5	BRK
993182.....	40445.68189	−1.3	PRN	6703882	45142.82667	5.6	BRK
1006414	40456.56544	−1.8	PRN	6703911	45142.85049	2.7	BRK
1052535	40494.50077	−3.0	PRN	6776586	45202.62678	2.4	BRK
1058606	40499.49424	−6.0	PRN	6777825	45203.64591	5.2	BRK
1059826	40500.49764	−12.2	PRN	6777910	45203.71582	5.1	BRK
1322888	40716.87108	13.0	PRN	6814301	45233.64805	11.9	...
1506118	40867.58094	9.5	PRN	7137774	45499.70943	8.8	...
1691426	41020.00004	11.4	PRN	7137999	45499.89447	6.9	...
1727900	41050.00050	7.9	PRN	7138945	45500.67255	5.3	...
1929276	41215.63570	2.1	PRN	7140355	45501.83226	1.6	...
1935321	41220.60785	5.6	PRN	7141528	45502.79699	−5.3	...
2153423	41400.00058	10.9	PRN	7142702	45503.76272	3.5	...
2360105	41570.00009	12.1	PRN	7146453	45506.84798	4.3	...
2396579	41600.00045	1.0	PRN	8937318	46979.86079	13.1	MHPG
2685684	41837.79420	−2.3	PRN	8938499	46980.83205	1.8	MHPG
2782994	41917.83332	−3.2	PRN	10645367	48384.75481	−3.0	...
2783959	41918.62701	−6.3	PRN	10646589	48385.75992	−2.8	...
2816814	41945.65080	−6.4	PRN	11121949	48776.74996	−5.2	...
2820402	41948.60201	−4.4	PRN	11973092	49476.82648	−4.5	...
3154811	42223.65909	−0.7	PRN	11974246	49477.77567	−3.7	...

[a] Cycle number calculated with respect to eq. (5).
[b] PRN = Patterson et al. 1978; BRK = Balachandran et al. 1983; MHPG = Martell et al. 1995.

dashed line in Figure 6 is the cubic ephemeris derived by fitting only the times of maxima after the gap and then extrapolating to earlier times. The early times of maximum are shown at three different locations in the $O-C$ diagram, corresponding to three different assumptions about the number of cycles that elapsed during the gap. The two cycle counts shown as solid and open circles in the diagram correspond to the "369 count" (*open circles*) and "370 count" (*filled circles*) discussed in PRN and Balachandran et al. (1983), and with the same counting convention, the cycle count shown as open squares would be called the "371 count."

Although PRN and Balachandran et al. (1983) both preferred the 370 count, their preference depended on the details of the weighting scheme and on the specific criteria used to decide between the counts. The new data show that the 370 count is, in fact, correct. As shown in Figure 6, the extrapolated cubic ephemeris falls far from, and excludes, the 369 count. The 371 count is excluded because the cubic ephemeris for the 371 count yields a poor fit to the observed value of $\dot{P}$ before the gap; that is, a cubic ephemeris yields a poor fit to the slope of the early times of maxima in the $O-C$ diagram. A χ^2 analysis confirms these conclusions. The unweighted χ^2 of fits to all the data simultaneously is 5150 s^2 for the 369 count, 4180 s^2 for the 370 count, and 9969 s^2 for the 371 count, yielding a nearly conclusive preference for the 370 count. The cycle numbers listed in Table 4 correspond to the 370 count; the best-fitting

© American Astronomical Society • Provided by the NASA Astrophysics Data System

1995ApJ...454..447Z

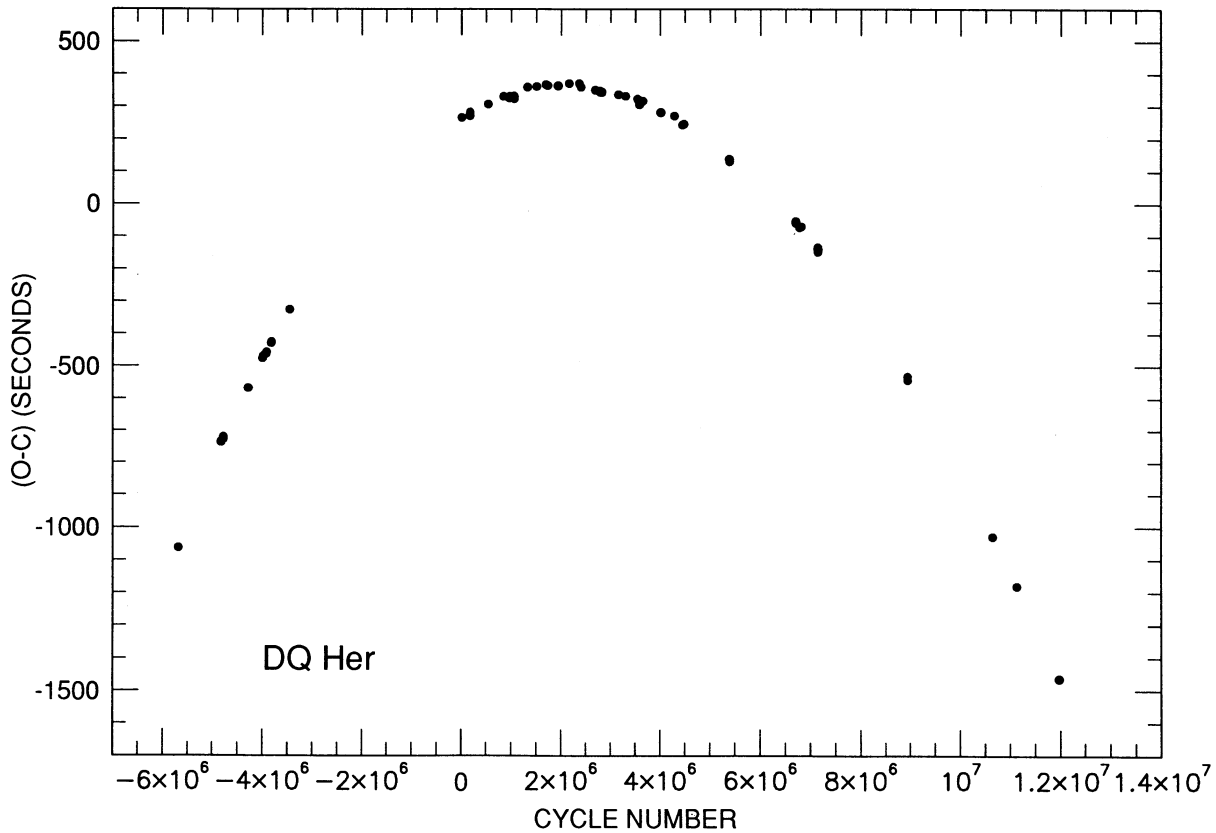

FIG. 5.—The $O-C$ diagram for maxima of the 71 s oscillation with respect to a linear ephemeris, showing that the oscillation period is decreasing rapidly. The cycle numbers for the maxima are given in Table 5.

cubic ephemeris for the 370 count is

$$T_{\max} = \text{HJED } 2{,}439{,}628.77177(\pm 0.00003) + (8.22518320 \pm 0.00000003) \times 10^{-4} E - (2.62 \pm 0.04) \times 10^{-16} E^2 + (2.8 \pm 0.1) \times 10^{-24} E^3 , \quad (5)$$

which is equivalent to

$$P = 71.0655828 \pm 0.0000003 \text{ s} , \quad (6)$$

$$\dot{P} = -(6.4 \pm 0.1) \times 10^{-13} \text{ s s}^{-1} , \quad (7)$$

$$\ddot{P} = (2.9 \pm 0.1) \times 10^{-22} \text{ s s}^{-2} . \quad (8)$$

Note that P, $\dot{P}$, and $\ddot{P}$ are the values at cycle zero in 1967. The residuals with respect to the cubic ephemeris are listed in Table 4 and plotted in Figure 7. The rms residual, ± 6.6 s, is substantially larger than the measurement error. Unlike the residuals of the times of eclipse, the residuals of the times of maxima do not follow any obvious systematic pattern.

The rotation period of the white dwarf in DQ Her is changing extremely rapidly. If the white dwarf is rotating as a solid body with constant radius, the rate of change of its rotational energy is $\dot{E} = I\omega\dot{\omega} \sim 2\ L_{\odot}$. Changes in the rotational periods of intermediate polars are usually ascribed to accretion torques. Even if we accept this interpretation, there are two reasons to believe that the spin period in DQ Her must, nevertheless, be near its equilibrium value. First, although $\dot{P}$ is large, the timescale for the period change $\tau_P = P/\dot{P}$ is not particularly short, $\tau_P = 3.5 \times 10^6$ yr. This should be compared to $\tau_P = 3.8 \times 10^6$ yr for EX Hya and $\tau_P = 4.1 \times 10^5$ yr for BG CMi (Hellier & Sproats 1992; Patterson & Thomas 1993). Second, the second derivative of the period is so large that $\dot{P}$ will go to zero, leaving a constant period, on the remarkably short timescale $\tau_P = \dot{P}/\ddot{P} = 70$ yr. Since the rotation period is near equilibrium, the magnetic moment of the white dwarf in DQ Her can be determined from

$$\omega_s = 0.041 P_{1000}^{-1} \dot{M}_{17}^{-3/7} M_1^{-5/7} \mu_{32}^{6/7} , \quad (9)$$

where μ_{32} is the magnetic moment in units of 10^{32} G cm^3 (Norton & Watson 1989). Adding $\omega_s = \omega_{\text{crit}} \approx 0.6$, $\dot{M} = 5 \times 10^{-9}\ M_{\odot}$ yr^{-1}, $P = 71.06$ s, and $M_1 = 0.60\ M_{\odot}$ (Horne et al. 1993), we find $\mu_{32} = 1.2$, in unsurprisingly good agreement with earlier estimates (Patterson 1994). However, as we will show later, the rotation period is probably 142 s, not 71 s, so the magnetic moment is really a factor of 2.2 larger $\mu_{32} = 2.7$.

Caution should be used in attributing the rate of change of the rotation period to accretion torques, however. It has been remarked that the timescale for equilibration of the rotational period, $\tau_P = 70$ yr, is comparable to the time since DQ Her erupted in 1934, suggesting a connection between the two. Katz (1975) showed that change in the structure of the white dwarf as it cools and shrinks will alter its moment of inertia and thus its rotation period. His calculations suggest that the magnitude of this mechanism is large enough to complete with accretion torques in changing the rotation rate.

Finally, we have searched for other periodicities in the light curve by calculating power spectra of all our data. The only

© American Astronomical Society • Provided by the NASA Astrophysics Data System

1995ApJ...454..447Z

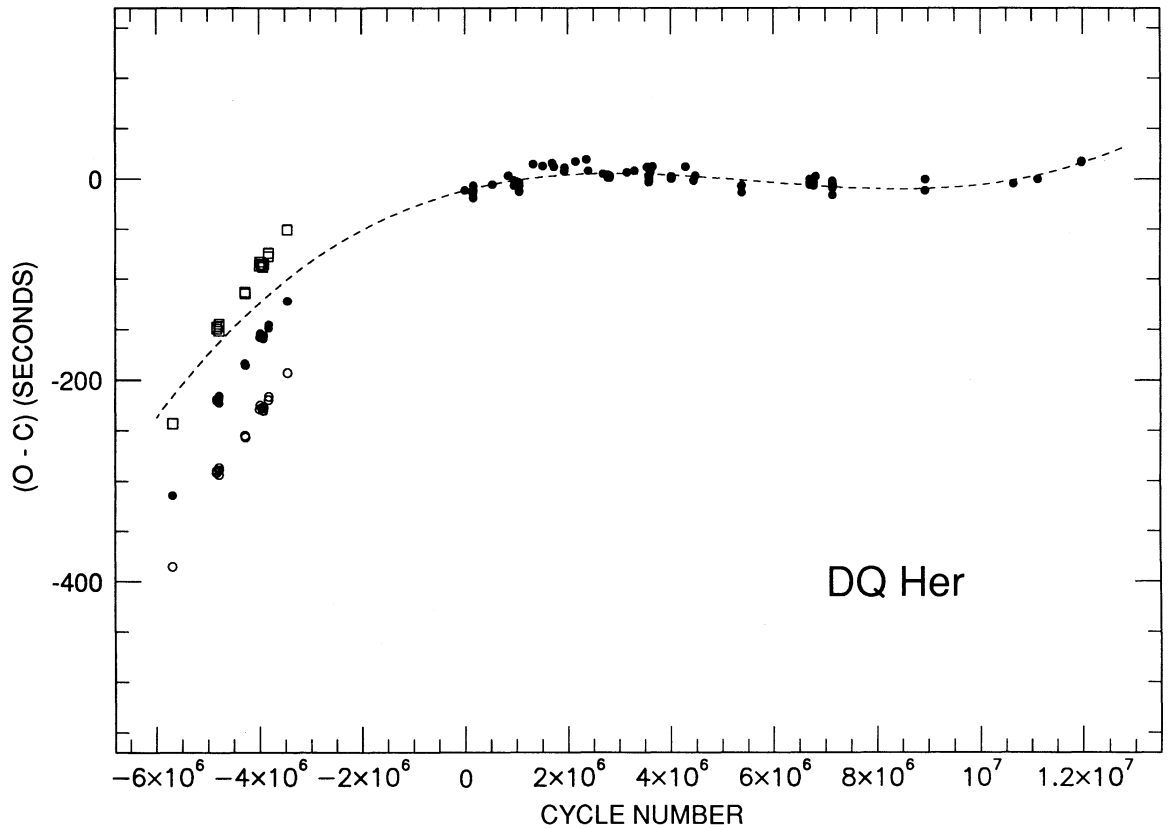

FIG. 6.—The $O-C$ diagram for maxima of the 71 s oscillation with respect to a quadratic ephemeris derived by fitting only times of maxima after the gap (cycles 0 and greater). A simple quadratic ephemeris is inadequate to describe the times of maxima. The dashed line is the cubic ephemeris derived by fitting only times of maxima after the gap; it has been extrapolated to earlier maxima. Residuals for the maxima before the gap are repeated three times, corresponding to three different cycle counts during the gap. Solid circles correspond to the 369 count, open circles correspond to the 370 count, and open squares correspond to the 371 count.

significant peak in the power spectra was at 71 s and we found no excess power at 142.1 s, twice the 71 s period. We also folded the light curves at a 142 s period but found no significant features in any color.

4. THE PHASE AND AMPLITUDE OF THE 71 SECOND OSCILLATION DURING ECLIPSE

It is always necessary to heavily process the light curves of DQ Her by averaging or digital filtering to measure the phase and amplitude of the 71 s oscillation accurately, and heavy processing is even more necessary during eclipse, when the amplitude becomes very small. All previous attempts to measure the amplitude and phase of the oscillation during eclipse have used the same basic method: the amplitude and phase are extracted from successive segments of an individual light curve, which may have been subjected to preprocessing, and then the amplitudes and phases from the individual light curves are averaged to give final amplitudes and phases. This method suffers from a serious drawback. If the errors in the measured phases in the individual light curves are large, the cycle count becomes uncertain and the phases can no longer be averaged properly. To keep the phase error small and avoid this problem, one must average over many cycles in the light curve. Unfortunately, both the amplitude and phase of the 71 s oscillation change rapidly during the eclipse, so averaging over many cycles degrades the time resolution, leading to ambiguous results.

In the present paper we reverse the order in which we analyze the data: We first fold the light curves in orbital phase to create a mean light curve and then extract the phase and amplitude of the 71 s oscillation from this mean light curve. Since the 71 s oscillation would cancel out in the mean light curve if the light curves were folded precisely at the orbital period, we shift the individual light curves by up to ± 35.5 s ($=0.5 \times 71.06$ s) before folding to make the 71 s oscillation add constructively. This procedure reduces the flickering, scintillation, and photon counting noise in the mean light curve while preserving the amplitude and relative phase of the oscillation. All features in the orbital light curve except the 71 s oscillation are smeared by ± 35 s but the smearing is a minor effect since the eclipse lasts nearly 1 hr and has no sharp features.

An issue that arises in this method is how to determine the amount by which the light curves should be shifted before folding. We have tried two ways to determine the shifts. The first is to measure the phase of the 71 s oscillation in each light curve at some fiducial orbital phase and then shift the light curve according to the measured oscillation phase. The second is to calculate the phase of the 71 s oscillation from its ephemeris (eq. [5]) and then shift the light curve according to the calculated phase. Both these ways have much to recommend them, and neither is clearly superior. Fortunately, they give essentially identical results. All the results given in this paper are for shifts calculated from the ephemeris.

This method of analyzing the light curves is so effective that

© American Astronomical Society • Provided by the NASA Astrophysics Data System

1995ApJ...454..447Z

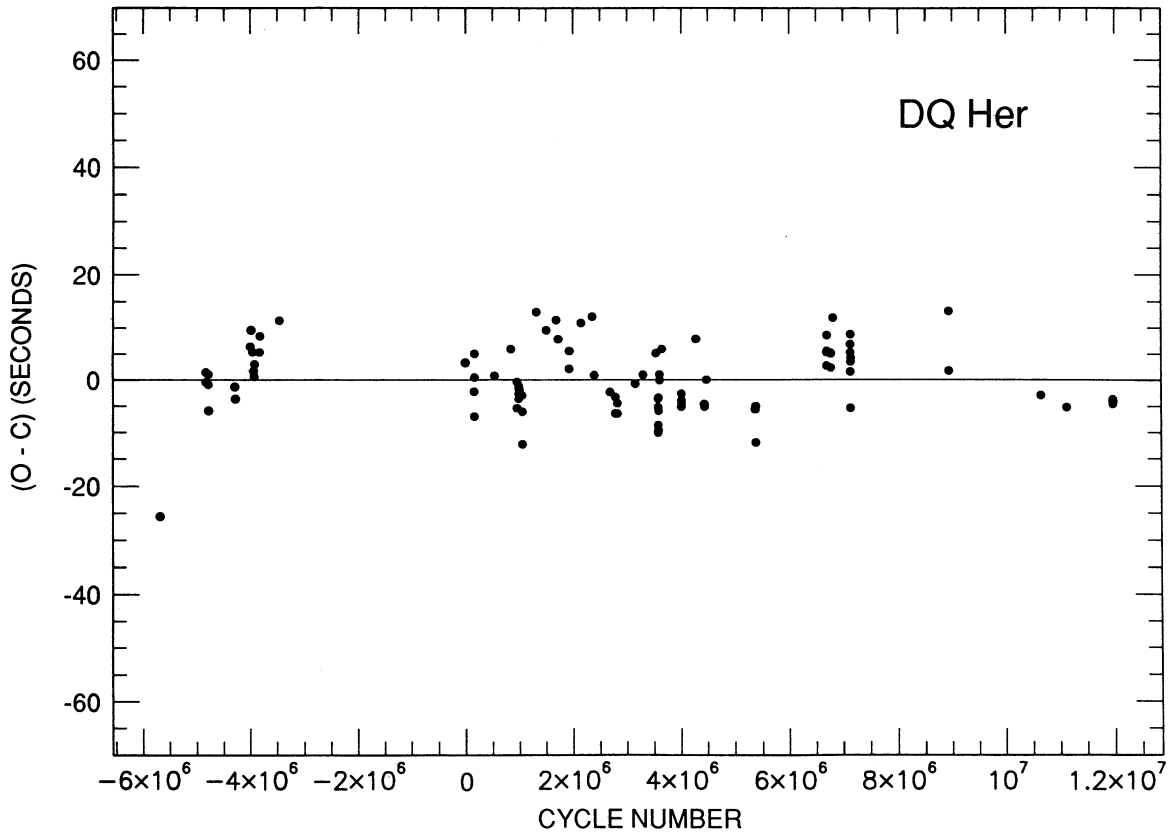

FIG. 7.—The $O-C$ diagram for maxima of the 71 s oscillations with respect to the best-fit cubic ephemeris. The times of maxima have an rms residual of ± 6.6 s.

we have dispensed altogether with complicated averaging or digital filtering schemes for extracting the phase and amplitude of the 71 s oscillation. After the mean light curve has been formed, the remaining analysis consists only of (1) removing the mean eclipse light curve from the data by subtraction to isolate the light curve of the 71 s oscillation, and (2) fitting a sine curve with length $n \times 71.06$ s to successive segments of the light curve, where n is an integer. Forcing n to be an integer minimizes spectral leakage from any residual noise in the light curve.

The upper four panels of Figure 8 show the folded U, B, V, and R light curves after the mean eclipse light curves have been subtracted. The fifth panel in the figure shows the light curve calculated by summing the U, B, V, and R light curves from each run to create a white-light light curve, and then folding all the white-light light curves at the orbital period. The improvement in the signal-to-noise ratio in the folded white-light light curve is substantial but somewhat less than expected because the flickering noise is highly correlated throughout the visual spectrum (note the similarity of the noise in all four colors near orbital phase -0.055) and the noise in the folded white-light light curve is dominated by flickering. The bottom panel of Figure 8 shows the folded B light curve for comparison.

Figure 9 shows the amplitude and phase of the 71 s oscillation in the folded white-light light curve as a function orbital phase; the white-light light curve from run 302 is shown for comparison. The amplitude and phase were measured by fitting a three-cycle sine curve to the mean light curve, advancing the sine curve one cycle between fits. The measured amplitude of the oscillation, which has been normalized to a mean of 100 in the figure, has large fluctuations at orbital phases far from eclipse because few light curves have been included in the sum light curve at those phases, but near eclipse, where more light curves have been included in the average, the fluctuations are much smaller and the measured amplitudes are reliable. The amplitude is larger than average at the beginning and end of the eclipse and drops smoothly to less than 10% of its uneclipsed average near mid-eclipse. The exact time of minimum amplitude occurs about 70 s after eclipse minimum and, if the amplitude drops to zero, it does so for no more than about three cycles at mid-eclipse.

The phase of the 71 s oscillation, shown in the upper panel of Figure 9, has been arbitrarily set to 0° at orbital phase 0.5. The oscillation phase shows large fluctuations at orbital phases far from eclipse, again because few light curves are included in the average, but with the likely exception of the three points near mid-eclipse the measured phases during eclipse are reliable. The external error of the phases, determined from the scatter of the measured phases immediately after eclipse, is $\pm 8°$ and, with the exception of the three points near mid-eclipse, increases only to $\pm 18°$ during eclipse. The oscillation phase increases smoothly by at least 100° during eclipse ingress, then jumps abruptly by $\sim 120°$ at mid-eclipse, and then climbs smoothly by another 140° to end at $+360°$ during eclipse egress. The abrupt jump, like the time of minimum amplitude, occurs about 1 minute after eclipse minimum. Since there is an ambiguity in the cycle count during the abrupt jump, we have also shown the phases after eclipse shifted down by one cycle.

According to PRN, the phase shift is less than $\pm 90°$. The difference between their results and ours is partly the result of

© American Astronomical Society • Provided by the NASA Astrophysics Data System

1995ApJ...454..447Z

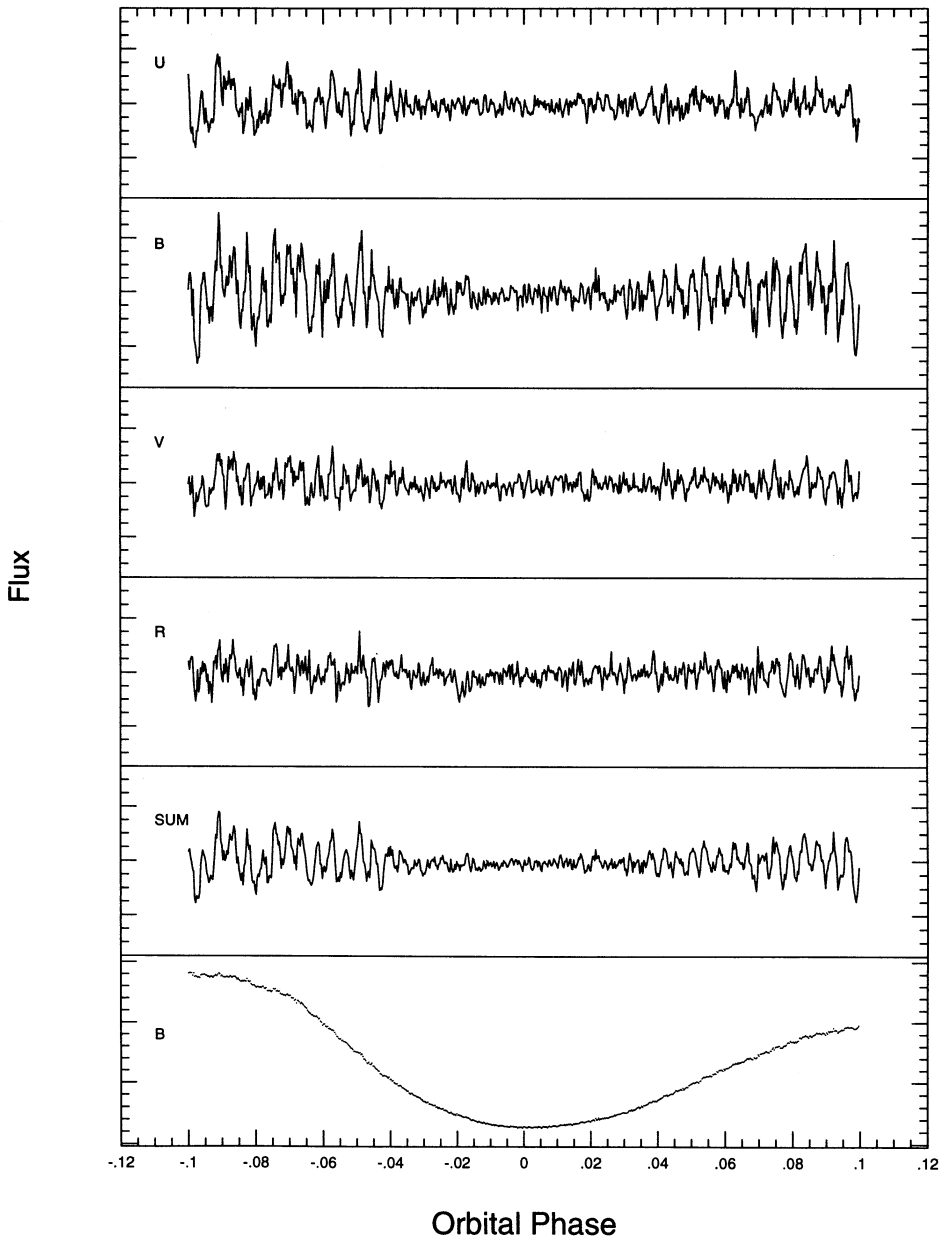

FIG. 8.—The bottom panel is the mean B light curve of DQ Her. The upper four panels show the folded U, B, V, and R light curves after the mean eclipse light curve in each color has been subtracted. The fifth panel shows the light curve calculated by summing the U, B, V, and R light curves of each run to create a white-light light curve, then folding all the white-light light curves at the orbital period. The 71 s oscillation is visible in the folded white-light light curve to within ± 0.02 in orbital phase of mid-eclipse.

our improved method for analyzing the data, but part of the difference is also caused by real changes in the properties of DQ Her. These changes show most clearly in the amplitude and phase of the oscillation outside of eclipse. PRN found that both the amplitude and the phase of the oscillations varied systematically with orbital phase. The amplitude varied by a factor of ~ 2.5, reaching a maximum between orbital phases 0.2 and 0.3, and the phase was systematically retarded by $\sim 30°$ between orbital phases -0.4 and -0.1. Although our new measurements are not very accurate at orbital phases far from eclipse, their accuracy is high enough to show that the systematic variations are much smaller or not present in the new data. The amplitude varies by less than 50% and the phase variation, if present at all, is less than 20°.

For completeness we show the amplitude and phases of the oscillation in U, B, V, and R as a function of orbital phase in Figures 10 and 11. The figures give little new information except that the behavior of the 71 s oscillation is not strikingly different in the four colors. The mean fractional semi-amplitudes of the 71 s oscillation in the four passbands are $\Delta U/U = 0.010 \pm 0.001$, $\Delta B/B = 0.012 \pm 0.001$, $\Delta V/V = 0.011 \pm 0.001$, and $\Delta R/R = 0.009 \pm 0.001$. Thus, the oscillation is significantly redder than the mean color of DQ Her in $U-B$ but bluer in $B-V$ and $V-R$. This differs some-

© American Astronomical Society • Provided by the NASA Astrophysics Data System

1995ApJ...454..447Z

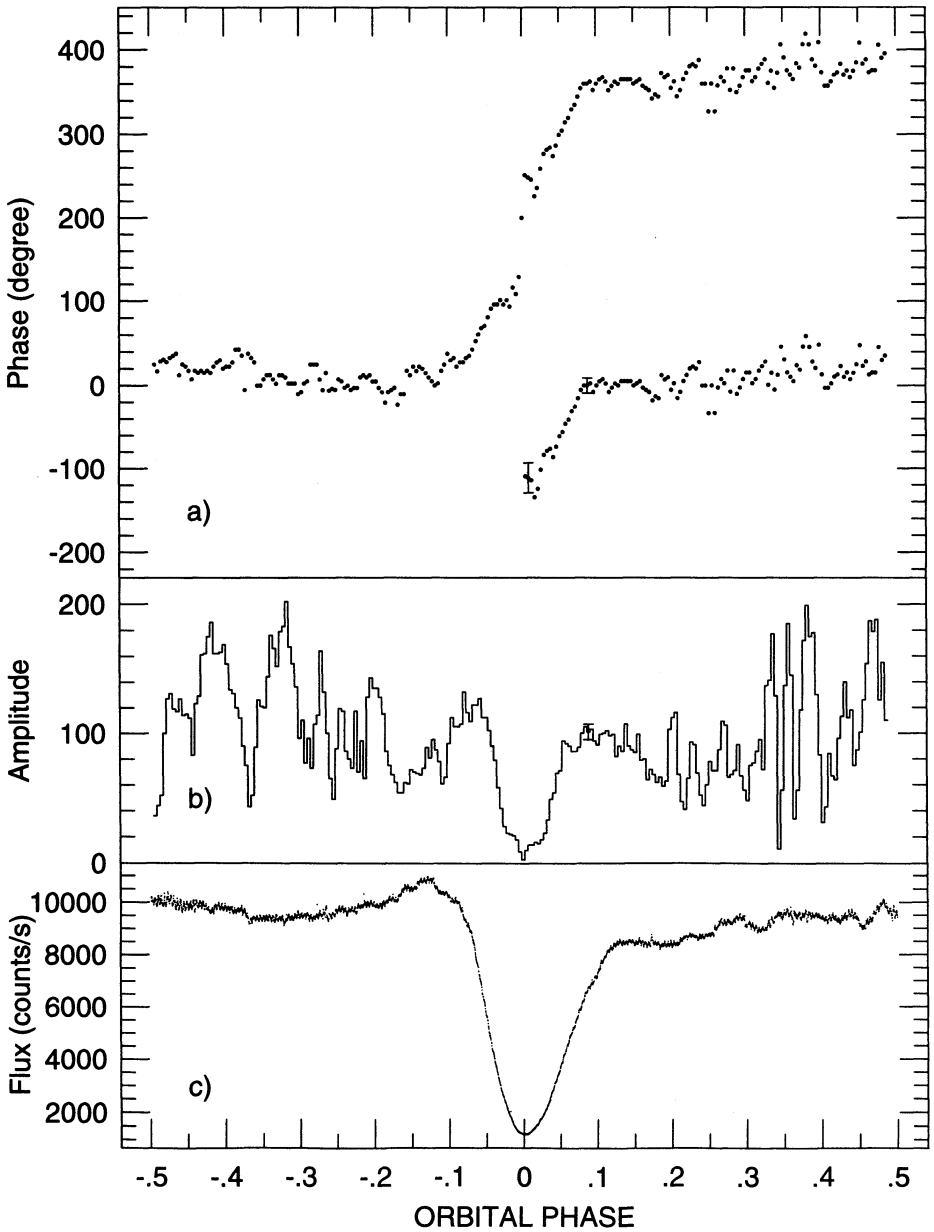

FIG. 9.—The amplitude and phase of the 71 s oscillation as a function of orbital phase in the summed (white-light) light curve; the white-light light curve during run 302 is shown for comparison. The amplitude and phase were measured by fitting a three-cycle sine curve to the mean light curve, advancing the sine curve by one cycle between fits. The phase of the 71 s oscillation has been arbitrarily shifted vertically to be near 0° before eclipse; the amplitude has been normalized to a mean of 100.

what from the result of PRN, who concluded that the colors of the oscillation were nearly the same as the mean colors of DQ Her.

5. ONE BEAM OR TWO? 71 SECONDS OR 142?

Although the rotating white dwarf must be the original source of the 71 s oscillation, the long duration of the phase shift demonstrates that the observed oscillation comes not from the white dwarf, but from the accretion disk. In the standard model for the phase shift (e.g., Petterson 1980), the accretion disk is illuminated by a beam or beams of radiation from the rotating white dwarf, which creates a rotating pattern of brighter and darker regions on the disk. During eclipse ingress, the rotating pattern is progressively occulted, so that the pattern reaches peak visibility earlier or later than when it is unocculted. Since the white dwarf must be rotating in the prograde direction, the positive sign of the phase shift demonstrates that the oscillations are seen primarily or only from the back of the accretion disk. The orbital inclination of DQ Her must be close to 90° so that the accretion disk and its rim, which are slightly flared, can block flux from the front of the disk and the white dwarf.

It has not been established conclusively whether the disk is illuminated by one or two beams, nor whether the rotation

© American Astronomical Society • Provided by the NASA Astrophysics Data System

1995ApJ...454..447Z

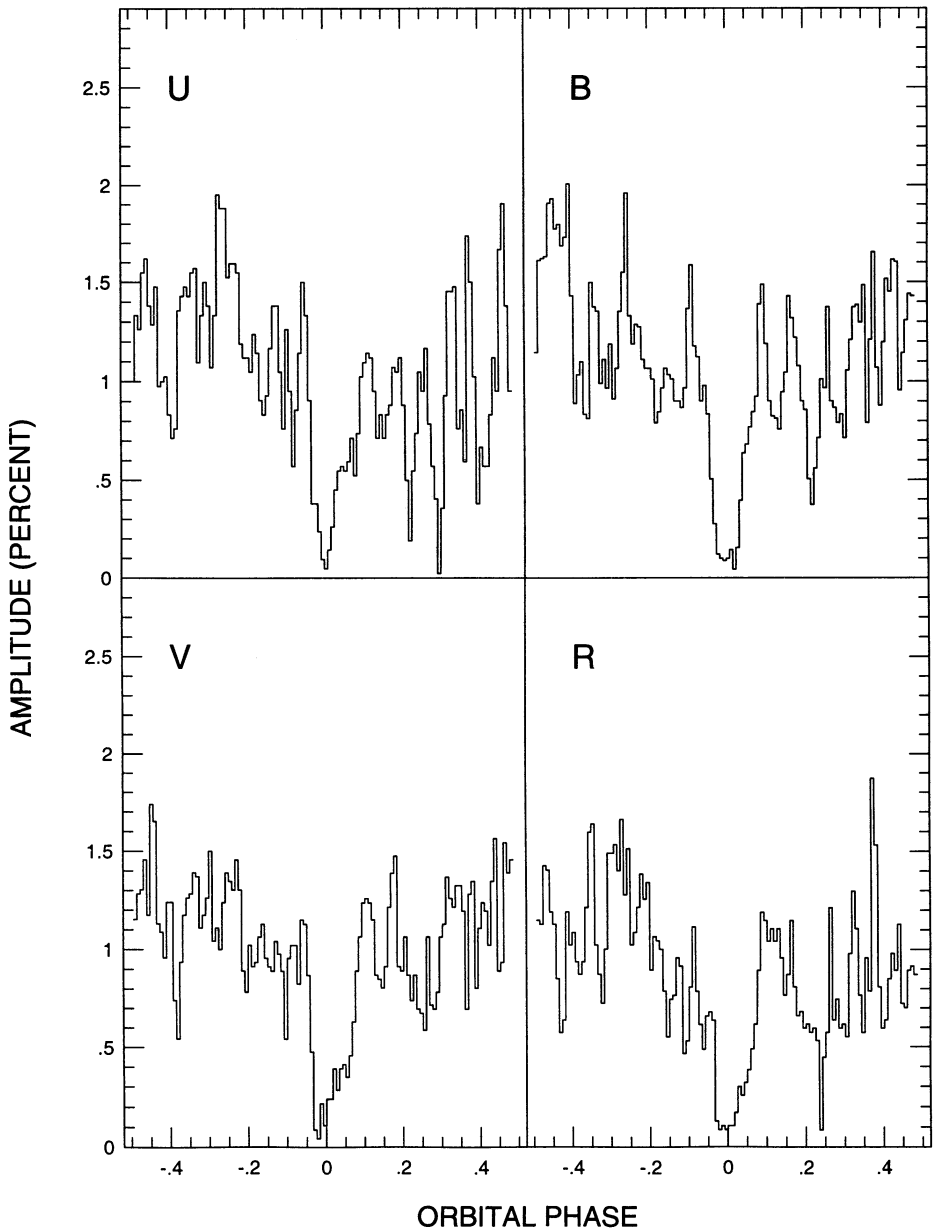

FIG. 10.—The amplitude of the 71 s oscillation as a function of orbital phase in the folded U, B, V, and R light curves. The amplitudes were measured by fitting a five-cycle sine curve, advancing the sine curve one cycle between fits. The amplitudes are plotted as a percentage of the mean flux in each color out of eclipse.

period of the pattern and thus of the white dwarf, is 71 s or 142 s. A 142 s modulation of any observed property of DQ Her would be strong evidence that the rotation period of the white dwarf is 142 s. Although there is some evidence for a 142 s photometric modulation (Nelson 1975; Schoembs & Rebhan 1989), the evidence has not been compelling and, equally often, as in our data, any modulation at 142 s is either absent or too weak to be detected (Kiplinger & Nather 1975; Nelson 1976). The detection of a 142 s modulation in the polarization of DQ Her by Kemp, Swedlund, & Wolstencroft (1974) and Swedlund, Kemp, & Wolstencroft (1974) had a low statistical significance and has never been confirmed.

The eclipse phase shift can be used to determine whether the brightness pattern rotating around the disk has one or two bright regions. The details of the phase shift depend on the geometry of DQ Her, especially on the geometry of the accretion disk and on whether the eclipse is total or partial, but the phase shift for models with one bright region is always less than $\pm 90°$, while the phase shift for models with two bright regions can be up to $\pm 180°$. We invoke a model for the phase shift which is somewhat simpler than, for example, Chester's (1979) and Petterson's (1980), but which preserves all the essential features of the process. We assume that bright spots on the white dwarf illuminate the accretion disk so that the brightness distribution across the disk is given, when viewed perpendicularly to the disk, by

$$I(\psi, t) \propto \sin(\omega t - n\psi), \quad (10)$$

where ω/n is the rotation frequency of the white dwarf, ψ is the angular position on the disk, and $n = 1$ if the pattern has one

© American Astronomical Society • Provided by the NASA Astrophysics Data System

1995ApJ...454..447Z

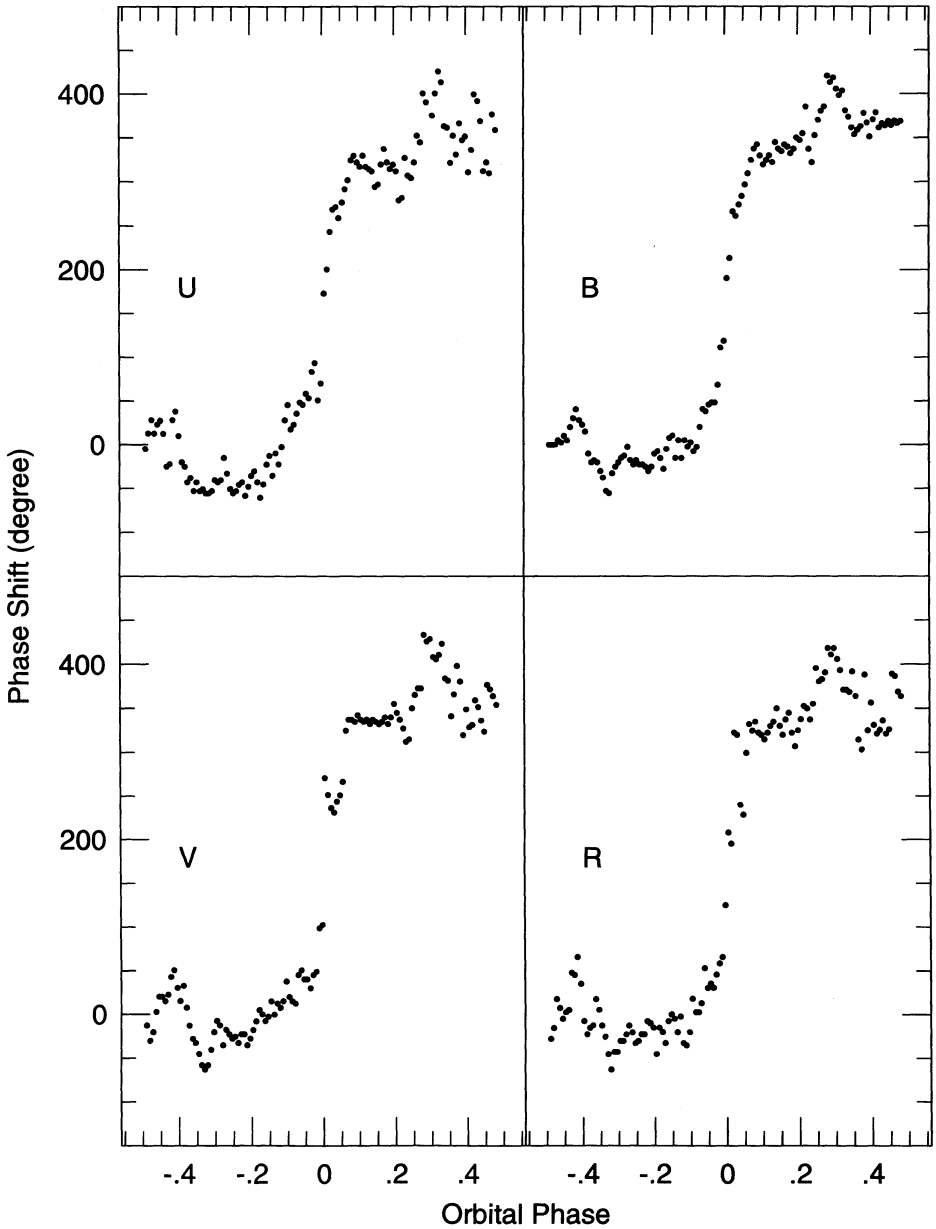

FIG. 11.—The phase of the 71 s oscillation as a function of orbital phase in the folded U, B, V, and R light curves. The phases were measured by fitting a five-cycle sine curve, advancing the sine curve one cycle between fits.

brightness maximum and 2 if it has two brightness maxima. For DQ Her $\omega = 2\pi/71.06\ \mathrm{s}^{-1}$. Thus, the brightness distribution looks somewhat like a spoked wheel rotating counterclockwise, one spoke for $n = 1$ and two spokes for $n = 2$.

When viewed at an orbital inclination i, the angular position on the disk is given by

$$\psi = \tan^{-1}\left(\frac{y/\cos i}{x}\right), \tag{11}$$

where (x, y) is a rectangular coordinate system on the plane of the sky, aligned such that the x axis is along the line of nodes and $\psi = 0$ is along the positive x-axis. We assume that the observed brightness of the tilted disk is given by

$$I(x, y, t) \propto \sin\psi \sin(\omega t - n\psi)\,. \tag{12}$$

The extra factor of $\sin\psi$ is a visibility function meant to simulate limb darkening and the vertical geometry of the disk; it serves much the same purpose as the factor $\theta(\eta)$ in Chester's equation (2). Following Chester (1979) and Petterson (1980), we will assume that the orbital inclination is large, so that the rim of the disk hides the front half of the disk, allowing only the back half to be seen. At these large inclinations, the limb of the eclipsing star can be approximated by a straight edge parallel to the y-axis. The flux from a disk of unit radius is then given by

$$F(t) \propto \int_{x_0}^{1}\int_{0}^{\cos i\sqrt{1-x^2}} I(x, y, t)\,dy\,dx = \alpha \sin\omega t + \beta\cos\omega t\,, \tag{13}$$

© American Astronomical Society • Provided by the NASA Astrophysics Data System

1995ApJ...454..447Z

where x_0 is related to the orbital phase ϕ_{orb} by

$$x_0 = \frac{a \sin \phi_{orb} \pm R_2}{R_D} . \quad (14)$$

R_D and R_2 are the radii of the disk and the occulting star, a is the separation between the centers of the white dwarf and the occulting star, and the sign of R_2 is positive for eclipse ingress and negative for egress. Thus, x_0 increases from -1 to 1 during eclipse ingress. A similar integral with limits running from -1 to x_0 holds for eclipse egress, and a partial eclipse can be simulated by the sum of the two integrals. The phase, ϕ, and amplitude, A, of the observed modulation is given in the usual way by $A = (\alpha^2 + \beta^2)^{1/2}$ and $\tan \phi = \beta/\alpha$. Note that although the orbital inclination is formally included in the model, the phase and relative amplitude of the modulation are, in fact, independent of the orbital inclination.

Figure 12 shows the amplitude and phase of the oscillation predicted by the model for a total eclipse. The amplitude of the oscillation in the two-spoke model is greater during eclipse ingress and egress than it it out of eclipse, but fades to zero at mid-eclipse. The phase shift in the two-spoke model can be described either as a smooth increase from 0° to 360° or, alter-

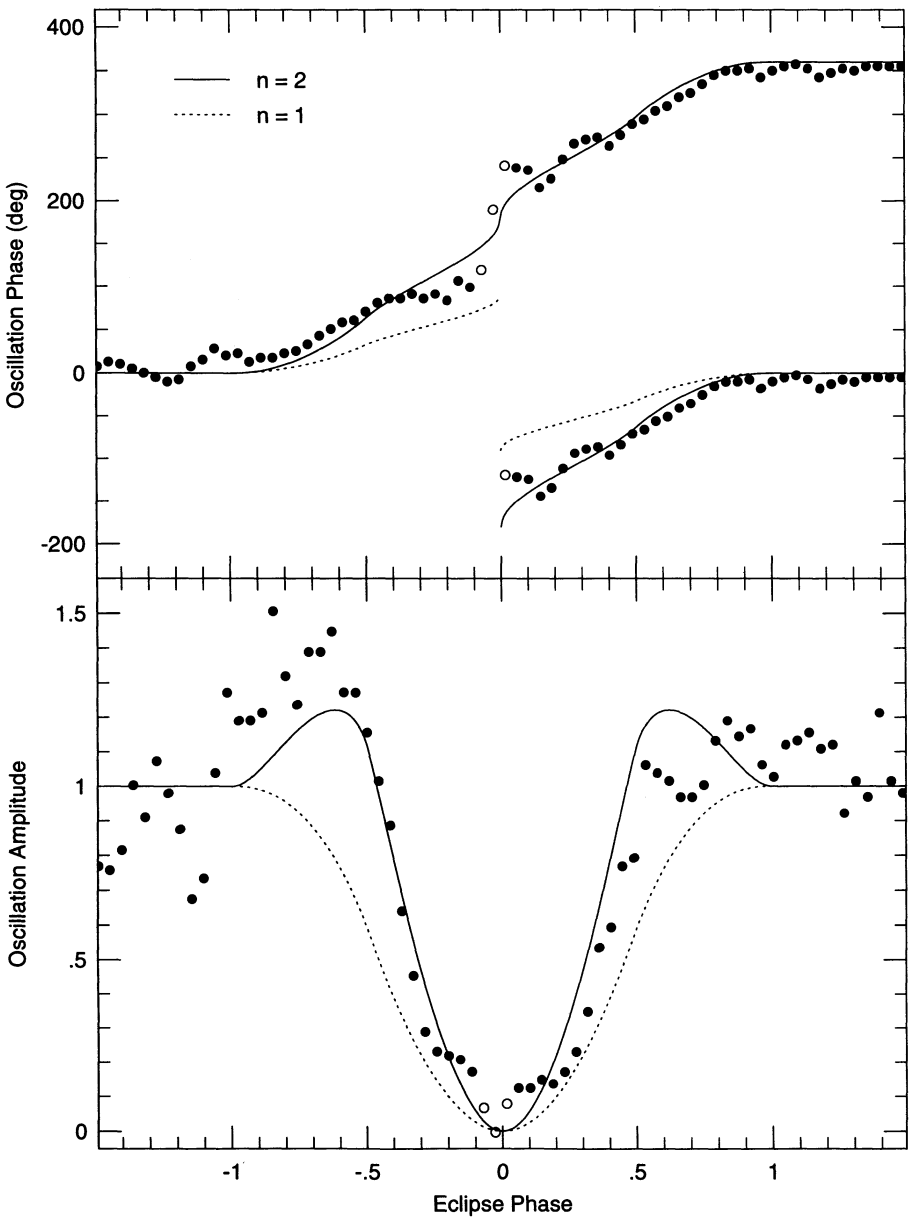

FIG. 12.—The solid and dashed lines give the phase (*top*) and amplitude (*bottom*) of the 71 s oscillation during a total eclipse as calculated from the model described in the text, where n is the number of spokes in the brightness pattern rotating around the disk. The eclipse phase has been defined to be -1 at the beginning of the eclipse and $+1$ at the end. The phase shift in the two spoke model can be described either as a smooth increase from 0° to 360°, or as a smooth increase to 180°, then an abrupt jump to $-180°$ followed by a smooth return to 0°. The two different descriptions are possible because the phase of the oscillation becomes indeterminate when its amplitude goes to zero at mid-eclipse. The amplitude is greater during eclipse ingress and egress but fades to zero at mid-eclipse. In the one spoke model, the phase increases smoothly to $+90°$, jumps abruptly to $-90°$, and then returns smoothly to 0°. The amplitude is always less during eclipse than out of eclipse. Dots represent the phase and amplitude of the oscillation in the folded, white-light light curve. They were measured by fitting a three-cycle sine curve to the light curve, advancing the sine curve by one cycle between fits. Three points near eclipse minimum have amplitudes consistent with zero and are shown as open circles.

© American Astronomical Society • Provided by the NASA Astrophysics Data System

1995ApJ...454..447Z

natively, as a smooth increase from 0° to 180°, then an abrupt jump to −180° followed by a smooth return to 0°. The two different descriptions are possible because the phase of the oscillation becomes indeterminate at mid-eclipse, when its amplitude goes to zero. The behavior of the one spoke model is much different. The phase increases only to +90°, jumps abruptly to −90°, and then returns smoothly to zero. Furthermore, the amplitude of the oscillation is always less during eclipse than out of eclipse.

The dots in Figure 12 are the observed amplitudes and phases of the 71 s oscillation in the folded white-light light curve. The data are the same as shown in Figure 9, except that the orbital phase has been scaled and shifted slightly to fit the model. The fit of the two spoke model to the data is remarkably good considering the simplicity of the model. Of particular note is the good agreement of the phases predicted by the two spoke model with the observed phases during eclipse egress. The one spoke model matches neither the slope nor, more importantly, the amount of the phase shift. The predicted and observed amplitudes of the oscillation also agree better with the two spoke model than with the one spoke model, but we place a heavier weight on the agreement in phase than the agreement in amplitude because the quality of the fit in amplitude depends strongly on the poorly known factor used to normalize the observed amplitudes.

We conclude that the brightness distribution across the accretion disk is a two-spoked pattern that revolves around the white dwarf with a period of 142 s and, therefore, that the rotation period of the white dwarf is also 142 s. The pattern of radiation emitted by the white dwarf is not, however, uniquely specified by the pattern it creates on the accretion disk. The white dwarf could, of course, be emitting radiation in two pencil beams, rather like the beams of a rotating lighthouse, but it is also possible that the white dwarf is emitting radiation in a single fan beam. If the radiation is emitted in a 360° fan roughly parallel to the surface of the white dwarf, perhaps by a source just above the surface of the white dwarf with an obscuring layer just above the source, the fan will intersect the accretion disk twice, in opposite directions, forming a two-spoked pattern on the disk.

Models invoking two pencil beams will have to contend with the near-perfect symmetry of the two beams. The upper limit placed by Kiplinger & Nather (1975) on any photometric modulation at 142 s forces the two spokes on the disk and thus the two beams from the white dwarf to have the same luminosity to within 6%. Furthermore, if the disk is optically thick or if it is optically thin only in a small region near the white dwarf, both beams must originate close to the equator to illuminate the disk equally. It will be difficult to achieve such a high degree of symmetry in a physically realistic model with two pencil beams. The requirements for symmetry are much more relaxed if the radiation is emitted as a single fan beam. The source of the beam can be anywhere on the white dwarf except near its rotation poles, and there are no constraints on the relative brightness of the two accretion poles as long as they are located roughly opposite each other on the white dwarf. We believe, therefore, that fan beam models are more likely to be correct.

6. SUMMARY

The revised eclipse ephemeris for DQ Her is given by equation (1). The upper limit on the rate of change of the orbital period limits the rate of mass transfer in the system to be less than, but not much less than $3.4 \times 10^{-9}\ M_{\odot}\ \mathrm{yr}^{-1}$. The revised ephemeris for the 71 s periodicity is given by equation (5). If the rotational period of the white dwarf is 142 s and if the rotation is near equilibrium, the magnetic moment of the white dwarf is $2.7 \times 10^{32}\ \mathrm{G\ cm}^3$.

The mean fractional semiamplitudes of the 71 s oscillation out of eclipse are $\Delta U/U = 0.010 \pm 0.001$, $\Delta B/B = 0.012 \pm 0.001$, $\Delta V/V = 0.011 \pm 0.001$, and $\Delta R/R = 0.009 \pm 0.001$. The oscillation is somewhat redder than the mean color of DQ Her in $U-B$, but bluer in $B-V$ and $V-R$. The large change in oscillation amplitude with orbital phase seen in earlier data is no longer present.

During eclipse, the phase of the 71 s oscillation increases smoothly by at least 100°, then jumps by ~120° at mid-eclipse, and then climbs smoothly by another ~140° to +360° during eclipse egress (see Fig. 9). The morphology of the phase shift is not measurably different in the four passbands. The amplitude of the oscillation is greater than its uneclipsed average during eclipse ingress and egress and drops smoothly to less than 10% of its uneclipsed average at mid-eclipse.

From the eclipse phase shift, we deduce that the brightness distribution across the accretion disk induced by beamed radiation from the white dwarf has two equal maxima on opposite sides of the disk somewhat like a two-spoked wheel, and that the pattern revolves around the white dwarf with a period of 142 s. We conclude, therefore that the rotation period of the white dwarf is 142 s.

REFERENCES

Africano, J. L., & Olson, E. C. 1981, PASP, 93, 130
Applegate, J. H., & Patterson, J. 1987, ApJ, 322, L99
Balachandran, S. 1983, Masters thesis, Univ. Texas at Austin
Balachandran, S., Robinson, E. L., & Kepler, S. O. 1983, PASP, 95, 653
Bianchini, A. 1990, in Accretion-Powered Compact Binaries, ed. C. W. Mauche (Cambridge: Cambridge Univ. Press), 149
Chester, T. J. 1979, ApJ, 230, 167
Hellier, C., & Sproats, L. N. 1992, Inf. Bull. Variable Stars, No. 3724
Horne, K., Welsh, W. F., & Wade, R. A. 1993, ApJ, 410, 357
Katz, J. K. 1975, ApJ, 200, 298
Kemp, J. C., Swedlund, J. B., & Wolstencroft, R. D. 1974, ApJ, 193, L15
Kiplinger, A. L., & Nather, R. E. 1975, Nature, 255, 125
Kraft, R. P. 1959, ApJ, 130, 110
Martell, P. J., Horne, K., Price, C. M., & Gomer, R. H. 1995, ApJ, 448, 380
McDermott, P. N., & Taam, R. E. 1989, ApJ, 342, 1019
Molnar, L. A. 1988, ApJ, 331, L25
Nelson, M. R. 1975, ApJ, 196, L113
———. 1976, ApJ, 209, 168
Norton, A., & Watson, M. G. 1989, MNRAS, 237, 715
Patterson, J. 1984, ApJS, 54, 448
———. 1984, PASP, 106, 209
Patterson, J., Robinson, E. L., & Nather, R. E. 1978, ApJ, 224, 570 (PRN)
Patterson, J., & Thomas, G. 1993, PASP, 105, 59
Petterson, J. A. 1980, ApJ, 241, 247
Pringle, J. E. 1975, MNRAS, 170, 633
Richman, H. R., Applegate, J. H., & Patterson, J. 1994, PASP, 106, 1075
Robinson, E. L., Shetrone, M. D., & Africano, J. L. 1991, AJ, 102, 1176
Robinson, E. L., et al. 1995, ApJ, 438, 908
Rubenstein, E. P., Patterson, J., & Africano, J. L. 1991, PASP, 103, 1258
Schneider, D. P., & Greenstein, J. L. 1979, ApJ, 233, 935
Schoembs, R., & Rebhan, H. 1989, A&A, 224, 42
Shafter, A. W., Wheeler, J. C., & Cannizzo, J. K. 1986, ApJ, 305, 261
Shara, M. M. 1989, PASP, 101, 5
Starrfield, S. 1989, in Classical Novae, ed. M. F. Bode & A. Evans (New York: Wiley), 39
Swedlund, J. B., Kemp, J. C., & Wolstencroft, R. D. 1974, ApJ, 193, L11
Walker, M. F. 1956, ApJ, 123, 68
———. 1958, ApJ, 127, 319
Warner, B. 1987, MNRAS, 227, 23
———. 1988, Nature, 336, 129
Warner, B., Peters, W. L., Hubbard, W. B., & Nather, R. E. 1972, MNRAS, 159, 321

© American Astronomical Society • Provided by the NASA Astrophysics Data System